

PERFORMANCE BOUNDS AND ALGORITHMS FOR TRACKING WITH A RADAR ARRAY

Mark R. Morelande, Sofia Suvarova and Bill Moran

Melbourne Systems Laboratory
Department of Electrical and Electronic Engineering
The University of Melbourne, Australia

email: m.morelande@ee.unimelb.edu.au, s.suvarova@ee.unimelb.edu.au, b.moran@ee.unimelb.edu.au

ABSTRACT

Target tracking using a radar array system is considered. A signal model which includes the effects of path loss, signal delay, Doppler shift and angle-of-arrival is adopted. The conventional approach to radar tracking assumes that the raw measurements are processed to produce a collection of candidate target detections. We propose a new approach in which the raw received measurements are used for tracking. Performance bounds and a simulation analysis of filters developed for each model demonstrate the performance gains which can be achieved by tracking with raw sensor measurements.

Keywords: Radar tracking, active arrays.

1. INTRODUCTION

This paper is concerned with the problem of tracking a target observed by a radar array system. Although radar signal processing has traditionally focussed on the use of receivers consisting of a single antenna [8], a receiver array allows more accurate estimation of range and Doppler and permits direction and, in principle, direction rate-of-change, to be estimated.

The most common approach to the radar tracking problem is to assume that the receiver measurements are processed to produce a set of candidate target measurements which are then supplied to the tracking algorithm [2]. This approach is adequate at high signal-to-noise ratios (SNRs). However, as the SNR decreases the tracking algorithm will be provided with an increasing number of false measurements, which must be resolved via data association [1], or, if detection thresholds are increased, reduced information regarding the target.

This paper investigates the possibility of tracking using the raw received measurements. First, performance bounds are derived for tracking with measurements obtained directly from the receiver and with measurements which have been processed to produce detections. The performance bound used here is the posterior Cramér-Rao bound (PCRB) [8] which lower bounds the mean square error of random parameter estimators. The PCRB is used to quantify the achievable performance gains from using received measurements directly in the tracker rather than detection measurements. Then, algorithms for tracking using the two measurement models are developed and compared. Tracking is performed using the unscented Kalman filter [6].

A similar idea was adopted in [10] although the approach and signal model differ considerably from those used here. Performance bounds for the static estimation problem were derived and analysed in [3] for a model similar to that considered here. The

model used here is more general as it includes the effects of path loss and time-varying direction of arrival, as suggested in [9].

The paper is organised as follows. The notation and signal models are given in Section 2. Posterior Cramér-Rao bounds are derived in Section 3 and the tracking algorithms are briefly described in Section 4. Section 5 contains a performance comparison.

2. NOTATION AND MODELING

The radar array tracking problem will be formulated as a nonlinear filtering problem. It is assumed that measurements are taken in discrete-time with t_k denoting the k th sampling instant, $k = 1, 2, \dots$. The difference $T_k = t_k - t_{k-1}$ will be referred to as the state sampling period.

The target is assumed to move in a plane. The target state at time t_k is denoted as $\mathbf{x}_k = [x_k, \dot{x}_k, y_k, \dot{y}_k, a_k, b_k]'$ where (x_k, y_k) is the target position in Cartesian coordinates, the dot notation denotes differentiation with respect to time and a_k and b_k are the real and imaginary parts of the target reflection coefficient. It is assumed that the target velocity and the reflection coefficients are subject to random variations. This leads to the dynamic model,

$$\mathbf{x}_k = \mathbf{F}_k \mathbf{x}_{k-1} + \mathbf{v}_k, \quad (1)$$

where $\{\mathbf{v}_k\}$ is a white Gaussian random process with covariance matrix \mathbf{Q}_k and

$$\mathbf{F}_k = \text{diag} \left(\mathbf{I}_2 \otimes \begin{bmatrix} 1 & T_k \\ 0 & 1 \end{bmatrix}, \mathbf{I}_2 \right), \quad (2)$$

$$\mathbf{Q}_k = \text{diag} \left(\mathbf{I}_2 \otimes \kappa_1 \begin{bmatrix} T_k^3/3 & T_k^2/2 \\ T_k^2/2 & T_k \end{bmatrix}, \kappa_2 T_k \mathbf{I}_2 \right) \quad (3)$$

with \otimes the Kronecker product and \mathbf{I}_m the $m \times m$ identity matrix.

The state is observed through one of the following two measurement models.

2.1. Received measurement model

Signals are transmitted at times t_k , $k = 1, 2, \dots$. The signals reflected from the target are received by a M -element array. It is assumed that the coordinate axes are selected so that the array is oriented along the x -axis. The received signals are converted to baseband and sampled with sampling period P . The n th sample of the received signal is, for $n = 0, \dots, N - 1$,

$$\mathbf{y}_k(nP) = \alpha(\mathbf{x}_k) s(nP - \tau(\mathbf{x}_k)) e^{j\nu(\mathbf{x}_k)nP} \mathbf{a}(nP; \mathbf{x}_k) + \mathbf{w}_{k,n}, \quad (4)$$

This work was supported by DARPA

where $\{\mathbf{w}_{k,n}\}$ is a zero-mean circular white Gaussian process with covariance matrix $\sigma^2 \mathbf{I}_M$ and s is the unit energy transmitted signal. The vector \mathbf{a} is the time-varying steering vector,

$$\mathbf{a}(t; \mathbf{x}) = \begin{bmatrix} 1 \\ e^{-j\bar{d}[\cos(\theta(\mathbf{x})) - \sin(\theta(\mathbf{x}))\dot{\theta}(\mathbf{x})t]} \\ \vdots \\ e^{-j(M-1)\bar{d}[\cos(\theta(\mathbf{x})) - \sin(\theta(\mathbf{x}))\dot{\theta}(\mathbf{x})t]} \end{bmatrix}, \quad (5)$$

where $\bar{d} = 2\pi d/\lambda$ with d the separation between the elements of the sensor array and λ the wavelength of the carrier signal. The target-related quantities appearing in (4) and (5) are defined as follows. Consider a state vector $\mathbf{x} = [x, \dot{x}, y, \dot{y}, a, b]'$. The received signal amplitude $\alpha(\mathbf{x})$ and delay $\tau(\mathbf{x})$ are

$$\alpha(\mathbf{x}) = \sqrt{E}(a + jb)/(r(\mathbf{x})\rho(\mathbf{x})), \quad (6)$$

$$\tau(\mathbf{x}) = [r(\mathbf{x}) + \rho(\mathbf{x})]/c, \quad (7)$$

where $r(\mathbf{x})$ and $\rho(\mathbf{x})$ are the distances between the target and the transmitter and receiver, respectively, E is the transmitted energy and c is the propagation speed. The Doppler shift applied to the signal is

$$\nu(\mathbf{x}) = 2\pi[\Omega(\mathbf{x}) + \omega(\mathbf{x})]/\lambda. \quad (8)$$

where $\Omega(\mathbf{x})$ and $\omega(\mathbf{x})$ are range rates between the transmitter and receiver, respectively. The angle of arrival and its time derivative are given by

$$\theta(\mathbf{x}) = \arctan[(y - \zeta)/(x - \xi)], \quad (9)$$

$$\dot{\theta}(\mathbf{x}) = [\dot{x}(\zeta - y) - \dot{y}(\xi - x)]/\rho(\mathbf{x})^2, \quad (10)$$

where (ξ, ζ) is the receiver position. The received signal samples are collected in the $NM \times 1$ vector

$$\mathbf{y}_k = [\mathbf{y}_k(0)', \dots, \mathbf{y}_k((N-1)P)']'. \quad (11)$$

The signal model (4) makes the standard narrowband assumptions in addition to the approximation [9]

$$\cos(\theta + \dot{\theta}t) \approx \cos(\theta) - \sin(\theta)\dot{\theta}t. \quad (12)$$

Eq. (12) is valid if $\dot{\theta}t$ is small over the surveillance duration. Note that the surveillance duration NP is much smaller than the state sampling period T_k .

2.2. Detection measurement model

The second measurement model assumes that the measurements \mathbf{y}_k have been processed in an optimal manner to produce estimates of the target parameters. In high noise scenarios there is a significant chance that the estimation procedure will produce false estimates. It is desired to reject such estimates. The optimal procedure would be to compare the likelihood ratio with a selected threshold [8]. Although this requires knowledge of the unknown target parameters it will be assumed here that this processing has been performed. It is assumed that the selected threshold is such that the probability of accepting a false estimate is negligible. This is reasonable in typical radar systems [5]. The process of rejecting unsuitable estimates can then be modelled by adopting a detection probability $P_D(k)$ which is the probability that an estimate will be accepted at the k th sample. Then, at time t_k a measurement is produced with probability $P_D(k)$ according to

$$\mathbf{z}_k = \mathbf{x}_k + \mathbf{e}_k, \quad (13)$$

where $\{\mathbf{e}_k\}$ is a zero-mean white Gaussian process with covariance matrix $\mathbf{R}(\mathbf{x}_k)$ with $\mathbf{R}(\mathbf{x}_k)^{-1}$ the Fisher information matrix (FIM) for the model (4) with \mathbf{x}_k a deterministic parameter. With probability $1 - P_D(k)$ no measurement is produced. The assumptions adopted here favour the detection measurement model since optimal detection and estimation cannot be performed in practice.

In the framework outlined in this section the tracking problem can be solved in an optimal manner, in the minimum mean square error sense, by recursively computing the posterior distribution of the state. This is not possible so sub-optimal techniques are required. One possibility will be described in Section 4.

3. DERIVATION OF THE PCRBS

The PCRBS provides a lower bound on the mean square error (MSE) of estimators of random parameters [8]. The PCRBS for radar tracking using the measurement models of Section 2 will be derived in this section.

3.1. Received measurement model

Assume that the target state \mathbf{x}_k evolves according to (1) and is observed through (4). The procedure of [7] can be used to recursively compute the PCRBS for estimators of \mathbf{x}_k . Assume that the estimator $\hat{\mathbf{x}}_{k-1}$ of \mathbf{x}_{k-1} conditional on measurements up to time t_{k-1} satisfies $\text{mse}(\hat{\mathbf{x}}_{k-1}) \geq \mathbf{J}_{k-1}^{-1}$. Then, $\text{mse}(\hat{\mathbf{x}}_{k-1}) \geq \mathbf{J}_k^{-1}$ where

$$\mathbf{J}_k = \mathbf{C}_k + \mathbf{D}_k - \mathbf{B}'_k(\mathbf{J}_{k-1} + \mathbf{A}_k)^{-1}\mathbf{B}_k, \quad (14)$$

with

$$\mathbf{A}_k = -\mathbb{E}[\nabla_{\mathbf{x}_{k-1}} \nabla'_{\mathbf{x}_{k-1}} \log p(\mathbf{x}_k | \mathbf{x}_{k-1})] = \mathbf{F}'_k \mathbf{Q}_k^{-1} \mathbf{F}_k, \quad (15)$$

$$\mathbf{B}_k = -\mathbb{E}[\nabla_{\mathbf{x}_{k-1}} \nabla'_{\mathbf{x}_k} \log p(\mathbf{x}_k | \mathbf{x}_{k-1})] = -\mathbf{F}'_k \mathbf{Q}_k^{-1}, \quad (16)$$

$$\mathbf{C}_k = -\mathbb{E}[\nabla_{\mathbf{x}_k} \nabla'_{\mathbf{x}_k} \log p(\mathbf{x}_k | \mathbf{x}_{k-1})] = \mathbf{Q}_k^{-1}, \quad (17)$$

$$\mathbf{D}_k = -\mathbb{E}[\nabla_{\mathbf{x}_k} \nabla'_{\mathbf{x}_k} \log p(\mathbf{y}_k | \mathbf{x}_k)]. \quad (18)$$

where ∇ is the gradient operator. The expectation (18) can be expanded as $\mathbf{D}_k = \mathbb{E}[\mathbf{\Lambda}(\mathbf{x}_k)]$ where the expectation is over the target state and $\mathbf{\Lambda}(\mathbf{x}_k) = \mathbb{E}[\nabla_{\mathbf{x}_k} \nabla'_{\mathbf{x}_k} \log p(\mathbf{y}_k | \mathbf{x}_k) | \mathbf{x}_k]$. It can then be shown that

$$\mathbf{\Lambda}(\mathbf{x}_k) = 2/\sigma^2 \sum_{n=0}^{N-1} \text{Re} \{ \nabla_{\mathbf{x}_k} \boldsymbol{\mu}_n(\mathbf{x}_k)^* [\nabla_{\mathbf{x}_k} \boldsymbol{\mu}_n(\mathbf{x}_k)]' \}, \quad (19)$$

where $*$ denotes conjugate transpose and, for a target state \mathbf{x} ,

$$\boldsymbol{\mu}_n(\mathbf{x}) = \alpha(\mathbf{x})s(nP - \tau(\mathbf{x}))e^{j\nu(\mathbf{x})nP} \mathbf{a}(nP; \mathbf{x}). \quad (20)$$

The gradient of $\boldsymbol{\mu}_n$ can be expanded as

$$\begin{aligned} \nabla_{\mathbf{x}} \boldsymbol{\mu}_n(\mathbf{x})' &= \nabla_{\mathbf{x}} \alpha \frac{\partial \boldsymbol{\mu}_n'}{\partial \alpha} + \nabla_{\mathbf{x}} \tau \frac{\partial \boldsymbol{\mu}_n'}{\partial \tau} + \nabla_{\mathbf{x}} \nu \frac{\partial \boldsymbol{\mu}_n'}{\partial \nu} \\ &\quad + \nabla_{\mathbf{x}} \theta \frac{\partial \boldsymbol{\mu}_n'}{\partial \theta} + \nabla_{\mathbf{x}} \dot{\theta} \frac{\partial \boldsymbol{\mu}_n'}{\partial \dot{\theta}}. \end{aligned} \quad (21)$$

The derivatives required in (21) can be found from (6), (7), (8)-(10) and (20) and the resulting expression for the gradient of $\boldsymbol{\mu}_n$ substituted into (19). The matrix \mathbf{D}_k is then found by taking the expectation of $\mathbf{\Lambda}(\mathbf{x}_k)$ over the target state \mathbf{x}_k . This cannot be found exactly but can be approximated by Monte Carlo simulation. Let $\mathbf{x}_k^1, \dots, \mathbf{x}_k^L$ denote a collection of target states generated according to (1). The matrix \mathbf{D}_k is then approximated as

$$\hat{\mathbf{D}}_k = 1/L \sum_{l=1}^L \mathbf{\Lambda}(\mathbf{x}_k^l). \quad (22)$$

3.2. Detection measurement model

PCRBs for tracking with a non-zero miss probability have been proposed in [4] and [11]. It was shown in [5] that the enumeration bound of [4] always provides a tighter bound than the computationally simpler information reduction factor bound of [11]. The enumeration bound will be adopted here. Define the detection indicator $d_k \in \{0, 1\}$ at time t_k with $d_k = 1$ meaning that the target is detected and $d_k = 0$ denoting otherwise. Let $d_{1:k} \in \{0, 1\}^k$ denote a sequence of detection of indicators. Then,

$$\text{mse}(\hat{\mathbf{x}}_k) \geq \mathbf{J}_k^{-1} = \sum_{d_{1:k} \in \{0, 1\}^k} \Pr(d_{1:k}) \mathbf{E}_k(d_{1:k})^{-1}, \quad (23)$$

where

$$\mathbf{E}_k(d_{1:k}) = \mathbf{C}_k + d_k \mathbf{E}[\mathbf{R}(\mathbf{x}_k)^{-1}] - \mathbf{B}'_k (\mathbf{E}_{k-1}(d_{1:k-1}) + \mathbf{A}_k)^{-1} \mathbf{B}_k, \quad (24)$$

$$\Pr(d_{1:k}) = \prod_{l=1}^k P_D(l)^{d_l} [1 - P_D(l)]^{1-d_l}. \quad (25)$$

The matrices \mathbf{A}_k , \mathbf{B}_k and \mathbf{C}_k are given in (15)-(17). Note that computation of the enumeration bound (23) requires the use of a PCRB recursion for each possible sequence of detections and misses. In practice, many of the sequences are unlikely and need not be included in (23). The FIM $\mathbf{R}(\mathbf{x}_k)^{-1}$ can be found as

$$\mathbf{R}(\mathbf{x}_k)^{-1} = -\mathbf{E} [\nabla_{\mathbf{x}_k} \nabla'_{\mathbf{x}_k} \log p(\mathbf{y}_k | \mathbf{x}_k)] = \mathbf{\Lambda}(\mathbf{x}_k), \quad (26)$$

where $\mathbf{\Lambda}(\mathbf{x}_k)$ is given in (19). The expectation required in (24) must be approximated as in (22).

It is interesting to compare the bounds (14) and (23). If $P_D = 1$ then the two bounds are identical. If $P_D < 1$, it can be shown using the results of [5] that the enumeration bound for the detection measurement model will exceed the bound for the received measurement model. This indicates that better performance can potentially be achieved using the received measurements directly rather than detections.

4. TRACKING WITH THE UNSCENTED KALMAN FILTER

Although superior performance is potentially possible using the received measurement model, it remains to be seen if the achievable improvements can be realised with practical algorithms. The basic filtering tool used here is the unscented Kalman filter (UKF) [6]. Although the detection measurement model of (13) is linear in the target state, the presence of measurement noise with a state dependent covariance matrix means that the Kalman filter is not the optimal Bayesian estimator.

Consider filtering using measurements from the received measurement model (4). The UKF represents the state estimate at time $k-1$ by a mean $\hat{\mathbf{x}}_{k-1|k-1}$ and covariance matrix $\mathbf{P}_{k-1|k-1}$. Since the dynamic equation (1) is linear and Gaussian the prediction step of the UKF can be performed exactly to give

$$\hat{\mathbf{x}}_{k|k-1} = \mathbf{F}_k \hat{\mathbf{x}}_{k-1|k-1}, \quad (27)$$

$$\mathbf{P}_{k|k-1} = \mathbf{F}_k \mathbf{P}_{k-1|k-1} \mathbf{F}'_k + \mathbf{Q}_k. \quad (28)$$

To perform the correction step, sigma points \mathcal{X}_k^i and weights w^i , $i = 1, \dots, s$ are selected. The sigma points and weights are such that the sample mean and covariance matrix are equal to $\hat{\mathbf{x}}_{k|k-1}$

and $\mathbf{P}_{k|k-1}$. Let $\mathbf{Y}_k = [\text{Re}\{\mathbf{y}_k\}', \text{Im}\{\mathbf{y}_k\}']'$. The expected measurements conditional on each sigma point are calculated as

$$\mathcal{Y}_k^i = [\text{Re}\{\boldsymbol{\mu}(\mathcal{X}_k^i)\}', \text{Im}\{\boldsymbol{\mu}(\mathcal{X}_k^i)\}']', \quad (29)$$

where $\boldsymbol{\mu}(\mathbf{x}) = [\boldsymbol{\mu}_0(\mathbf{x}), \dots, \boldsymbol{\mu}_{N-1}(\mathbf{x})]'$ with $\boldsymbol{\mu}_n(\mathbf{x})$ given in (20). The corrections to the predicted mean and covariance matrix are then computed as

$$\hat{\mathbf{x}}_{k|k} = \hat{\mathbf{x}}_{k|k-1} + \boldsymbol{\Psi}_k \mathbf{S}_k^{-1} (\mathbf{Y}_k - \hat{\mathbf{Y}}_k), \quad (30)$$

$$\mathbf{P}_{k|k} = \mathbf{P}_{k|k-1} - \boldsymbol{\Psi}_k \mathbf{S}_k^{-1} \boldsymbol{\Psi}'_k, \quad (31)$$

where

$$\hat{\mathbf{Y}}_k = \sum_{i=1}^s w^i \mathcal{Y}_k^i, \quad (32)$$

$$\mathbf{S}_k = \sigma^2 \mathbf{I}_{2NM} + \sum_{i=1}^s w^i (\mathcal{Y}_k^i - \hat{\mathbf{Y}}_k)(\mathcal{Y}_k^i - \hat{\mathbf{Y}}_k)', \quad (33)$$

$$\boldsymbol{\Psi}_k = \sum_{i=1}^s w^i (\mathcal{X}_k^i - \hat{\mathbf{x}}_{k|k-1})(\mathcal{Y}_k^i - \hat{\mathbf{Y}}_k)'. \quad (34)$$

The UKF recursion is potentially computationally expensive due to the inversion of the $2NM$ -dimensional matrix \mathbf{S}_k in (30). Two steps are taken to reduce computational expense. First, range gating based on the predicted target state is used to ignore samples which are unlikely to contain target reflections. Second, it is possible to perform the UKF correction without inverting \mathbf{S}_k . The equations demonstrating this have been omitted due to a lack of space. The recursion defined by (27), (28), (30) and (31) will be referred to as the received measurement UKF (RM-UKF).

The prediction step of the UKF recursion for the detection measurement model is identical to that used for the received measurement model. Recall the detection indicator d_k which takes the value one if the target is detected and is zero otherwise. After selecting sigma points as above, the correction step for the UKF recursion for the detection measurement model is

$$\hat{\mathbf{x}}_{k|k} = \hat{\mathbf{x}}_{k|k-1} + d_k \boldsymbol{\Psi}_k \mathbf{S}_k^{-1} (\mathbf{z}_k - \hat{\mathbf{x}}_{k|k-1}), \quad (35)$$

$$\mathbf{P}_{k|k} = \mathbf{P}_{k|k-1} - d_k \boldsymbol{\Psi}_k \mathbf{S}_k^{-1} \boldsymbol{\Psi}'_k, \quad (36)$$

where $\boldsymbol{\Psi}_k = \mathbf{P}_{k|k-1}$ and

$$\mathbf{S}_k = \mathbf{P}_{k|k-1} + \sum_{i=1}^s w^i \mathbf{R}(\mathcal{X}_k^i). \quad (37)$$

The recursion defined by (27), (28), (35) and (36) will be referred to as the detected measurement UKF (DM-UKF).

5. SIMULATION RESULTS

The performances of the two tracking methods are compared using Monte Carlo simulations. In this scenario the transmitter is located at (35, 0) and the receiver position is (90, 10). The transmitted signal is

$$s(t) = \frac{1}{\sqrt{2B+1}} \sum_{b=-B}^B \frac{\exp\{[j\vartheta - 1/(2\nu^2)](t-bA)^2\}}{(\pi\nu^2)^{1/4}} \quad (38)$$

Note that $\int |s(t)|^2 dt = 1$. The scaling parameter ν is selected to give an effective duration of $D = 7\nu = 250\text{ns}$. The chirp rate is

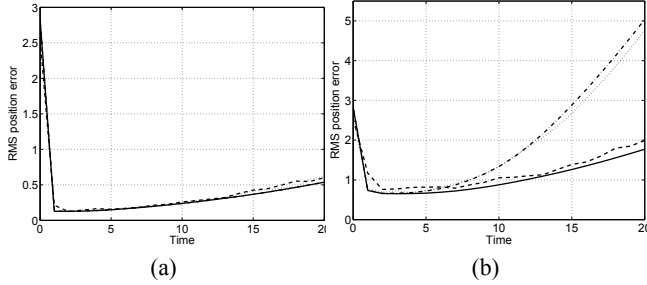


Figure 1: RMS position error of the RM-UKF (dashed) and DM-UKF (dotted) plotted against time for an SNR of (a) 10dB and (b) 0dB. The PCRB for the RM model is a solid line and the PCRB for the DM model is a dash-dot line.

$\vartheta = 3.2\pi \times 10^{14}$. The number of pulses is $2B + 1 = 21$ and the pulse repetition interval is $A = 100\mu\text{s}$. The observations are sampled with sampling period $P = 5\text{ns}$. The carrier frequency is 3GHz. The receiver has $M = 5$ elements with spacing $d = 0.4\text{m}$. The state sampling period is $T_k = 1\text{s}$ for $k = 1, \dots, K$ where $K = 20$ is the total number of sampling instants.

The initial target state is Gaussian with mean $[5, 9.65, 180, 11.5, 0.07, 0.07]'$ and covariance matrix $\text{diag}(4, 0.5, 4, 0.5, 0.1, 0.1)$. The target state evolves according to (1) with $\kappa_1 = 1/100$ and $\kappa_2 = 2 \times 10^{-5}$. Note that the target moves away from the transmitter and receiver so that the tracking problem becomes more difficult as the observation interval continues. For a received signal with amplitude α sampled with period P and embedded in noise with variance σ^2 , let $S = \alpha^2/(\sigma^2 P)$ denote the signal-to-noise ratio. For a false alarm probability P_{FA} , it can be shown that the detection probability for the likelihood ratio test is

$$P_D = 1 - \Phi \left[\Phi^{-1}(1 - P_{FA}) - \sqrt{2MS} \right], \quad (39)$$

where Φ is the distribution function of a standard Gaussian random variable. Here we fix $P_{FA} = 10^{-5}$. The detection probability used in the detection measurement model is calculated along the nominal state trajectory, i.e., the state trajectory with exact initial conditions and no process noise.

Since the amplitude of the received signal, and hence the SNR, vary throughout the observation interval, we use the average SNR of the measurements received for the nominal target trajectory as a single measure of the severity of the scenario. SNRs of 10dB and 0dB are considered. For an SNR of 10dB the transmitted signal is detected with probability very close to one at all time instants. For an SNR of 0dB the detection probability is close to one at the beginning of the observation interval but falls sharply as the target moves away from the transmitter and receiver. At the final sampling instant the detection probability is 0.135.

Figure 1 shows the RMS position errors for each SNR averaged over 100 Monte Carlo realisations. The PCRBs for each measurement model are also shown. For an SNR of 10dB the performances of the two filters and the PCRBs are almost identical. This is because measurements of the target are obtained with a probability very close to one in the detection model. A significant difference can be seen for the lower SNR of 0dB. As expected the PCRB for the RM model is much better than the PCRB for the DM model. The encouraging result is that the suboptimal RM-UKF is able to perform very close to the PCRB and significantly better than the DM-UKF.

6. CONCLUSIONS

We considered the problem of target tracking using a radar array. Our approach to the problem is based on passing the received sensor measurements directly to the tracking algorithm rather than following the customary approach of first processing these measurements to produce detections. Performance bounds were derived for both the received measurement and detection measurement models. This showed that the achievable performance with the raw measurement model is superior. A simulation analysis showed that it is possible for a filtering algorithm of reasonable computational expense to realise these performance gains.

7. REFERENCES

- [1] Y. Bar-Shalom and T. Fortmann, *Tracking and Data Association*. Academic Press, 1988.
- [2] Y. Bar-Shalom and X.-R. Li, *Estimation and Tracking: Principles, Techniques and Software*. Artech House, 1993.
- [3] A. Dogandzic and A. Nehorai, "Cramér-Rao bounds for estimating range, velocity and direction with an active array," *IEEE Transactions on Signal Processing*, vol. 49, no. 6, pp. 1122–1137, 2001.
- [4] A. Farina, B. Ristic, and L. Timmoneri, "Cramér-Rao bound for nonlinear filtering with $P_d < 1$ and its application to target tracking," *IEEE Transactions on Signal Processing*, vol. 50, no. 8, pp. 1916–1924, 2002.
- [5] M. Hernandez, B. Ristic, A. Farina, and L. Timmoneri, "A comparison of two Cramér-Rao bounds for nonlinear filtering with $P_d < 1$," *IEEE Transactions on Signal Processing*, vol. 52, no. 9, pp. 2361–2370, 2004.
- [6] S. Julier, J. Uhlmann, and H. Durrant-Whyte, "A new method for the nonlinear transformation of means and covariances in filters and estimators," *IEEE Transactions on Automatic Control*, vol. 45, no. 3, pp. 477–482, 2000.
- [7] P. Tichavský, C. Muravchik, and A. Hehorai, "Posterior Cramér-Rao bounds for discrete-time nonlinear filtering," *IEEE Transactions on Signal Processing*, vol. 46, no. 5, pp. 1386–1396, 1998.
- [8] H. Van Trees, *Detection, Estimation and Modulation Theory. Part 1, Detection, Estimation and Linear Modulation Theory*. John Wiley & Sons, 1968.
- [9] F. Vincent and O. Besson, "Estimating time-varying DOA and Doppler shift in radar array processing," *IEE Proceedings- Radar, Sonar and Navigation*, vol. 147, no. 6, pp. 285–290, 2000.
- [10] R. Zarnich, K. Bell, and H. Van Trees, "A unified method for measurement and tracking of contacts from an array of sensors," *IEEE Transactions on Signal Processing*, vol. 49, no. 12, pp. 2950–2961, 2001.
- [11] X. Zhang and P. Willett, "Cramér-Rao bounds for discrete-time linear filtering with measurement origin uncertainty," in *Proceedings of the Workshop on Estimation, Tracking and Fusion*, Monterey, California, 2001.